



15 **Abstract**

16 Observations of the ultraplankton ( $<5\mu\text{m}$ ) are presented from a 4 day mesoscale  
17 survey centred on the Porcupine Abyssal Plain (PAP) study site ( $49^{\circ}00'\text{N}$   $16^{\circ}30'\text{W}$ ),  
18 in July 2006. The organisms enumerated include two groups of phytoplankton,  
19 *Synechococcus* cyanobacteria, heterotrophic bacteria, large viruses and two size  
20 classes of heterotrophic protist. The dataset comprises over 400 samples from the  
21 mixed layer taken over a  $100\text{km} \times 100\text{km}$  area at a spatial resolution of typically 2-  
22 3km.

23 For phytoplankton and heterotrophic bacteria there is a clear bimodal structure  
24 to the histograms of abundance indicative of two distinct communities in the region.  
25 Using the strong bimodality of one of the phytoplankton groups' histogram as a basis,  
26 the dataset is split into two subsets, with roughly 200 points in each, corresponding to  
27 the two histogram peaks. Doing so provides evidence that *Synechococcus* and viruses  
28 may also have a bimodal structure. Correlations between all pairings of these 5  
29 organisms (both phytoplankton groups, *Synechococcus*, heterotrophic bacteria and  
30 viruses) are positive and quite high ( $r>0.7$ ). The two communities can therefore be  
31 characterised as high and low abundance. Although there is a coincidence of low  
32 abundances with high temperatures in the southwest corner of the region, where there  
33 was known to be an eddy present, the spatial distributions of these organisms over the  
34 whole region is poorly predicted by temperature (or salinity or density). Furthermore,  
35 the spatial distributions of heterotrophic protists are found to differ strongly from  
36 those of the other organisms, having a unimodal structure and no obvious large scale  
37 structure. The more random structure of the heterotrophs' spatial distribution  
38 compared to their prey is consistent with previous results from the continental shelf,  
39 but is demonstrated for the open ocean here for the first time.

40           Spatial variability is a large potential source of error in point samples, such as  
41 those comprising time series or transect cruises, unless a sufficient number of samples  
42 are taken. This large dataset is further used to provide guidance on the number of  
43 samples that would be required to estimate the mean abundance for the organisms  
44 accurately in this spatially variable region. Even if the bimodal structure was known  
45 initially, many of the organisms would require 10 or more samples to estimate the  
46 mean with 25% accuracy.

47 **1. Introduction**

48 The ultraplankton (plankton  $<5\mu\text{m}$  in size) are the most abundant organisms in the sea  
49 and play a fundamental role in marine biogeochemical cycles. Little is currently  
50 known of their spatial variability, however, particularly at the mesoscale (1-100km).  
51 In shelf seas there is evidence of very strong mesoscale spatial variability in  
52 ultraplankton (Martin et al. 2005). Furthermore, the spatial distributions of  
53 heterotrophs is markedly different from that of their prey there (Martin et al. 2008).  
54 Although there are some mesoscale datasets from the open ocean (e.g. Zubkov &  
55 Quartly, 2003) none to date have been adequate to ascertain whether the shelf sea  
56 phenomena are more general.

57 In June and July of 2006, RRS Discovery conducted a month long  
58 multidisciplinary cruise centred on the Porcupine Abyssal Plain study site ( $49^{\circ}50'N$   
59  $16^{\circ}30'W$ ). Towards the end of the cruise an intensive 4 day mesoscale survey of the  
60 area was conducted. During this survey ultraplankton samples were taken from the  
61 mixed layer, with typically 2-3km between samples. This provides a high resolution  
62 map of ultraplankton in the area, at such a level of taxonomic detail that two size  
63 classes of heterotrophic protist were separately counted as well as a range of their  
64 prey including two types of phytoplankton, *Synechococcus* cyanobacteria,  
65 heterotrophic bacteria and large ( $>0.2\mu\text{m}$ ) viruses. All the numerically dominant  
66 representatives of the ultraplankton predator-prey system were mapped.

67 This paper presents the results of that survey. It also uses this large dataset to  
68 offer practical guidance on the number of samples that need to be taken to avoid  
69 spatial variability leading to large errors in estimates of the mean abundance of  
70 organisms for this area. The high-resolution survey described here is one of very few  
71 yet conducted on ultraplankton (Jacquet et al., 2002; Zubkov & Quartly, 2003). Most

72 surveys must satisfy themselves with a much smaller number of data points. It is  
73 therefore germane to ask how many points it would be necessary to sample to obtain  
74 accurate estimates of the mean abundance of the various ultraplankton groups in a  
75 spatially variable region.

76

## 77 **2. Methods**

78

### 79 *2.1 Flow cytometry*

80 The mesoscale survey took 4 days, with each day devoted to surveying one of the  
81 quadrants, shown in Figure 1. Samples were taken for analysis from the non-toxic  
82 surface water supply every 12 mins giving a spatial resolution of typically 2-3 km.  
83 The intake for the non-toxic supply is at a depth of 6 m and hence well within the  
84 mixed layer (typically 20-30m throughout the cruise). Samples (2 x 2.4 ml) were  
85 automatically collected into polypropylene flow cytometry tubes (Fisher,  
86 Loughborough, UK) and fixed with 1% paraformaldehyde (PFA) using a Miniprep-60  
87 autosampler (Tecan, Reading, UK). Absolute concentrations of microbes were  
88 determined by flow cytometry (FACSort, Becton Dickinson Biosciences, Oxford,  
89 UK). Microbes were stained with SYBR Green I DNA stain (Sigma-Aldrich, Poole,  
90 UK), 1:5000 final dilution of initial stock, in the presence of potassium citrate, 30 mM  
91 final concentration, in the dark at +4°C for 2 – 4 h (Marie et al. 1997; Zubkov et al.,  
92 2007). A yellow-green 0.5 µm bead (Fluoresbrite Microparticles, Polysciences,  
93 Warrington, USA) concentration standard was added at known dilution to determine  
94 absolute cell concentrations (Zubkov & Burkill, 2006).

95

96 The two phytoplankton groupings were characterised by size and fluorescence. For  
97 simplicity they will be referred to as large orange fluorescence phytoplankton (LOP)  
98 and picophytoplankton (PPH). Regarding the former, dinoflagellates and *Mesodinium*  
99 are far too rare to be counted by flow cytometry. Therefore, they are most likely to be  
100 small (~ 3-8 $\mu$ m) Cryptophytes. Out of caution we simply refer to them as LOP. In  
101 addition to phototrophs and heterotrophic bacteria, heterotrophic protists and viruses  
102 were also enumerated (Zubkov et al. 2004; Zubkov et al. 2007). The two groupings of  
103 heterotrophic protists will be referred to simply as small (SHE) and large (LHE)  
104 heterotrophic protists. As the survey enumerated all numerically significant organisms  
105 in this size range it therefore represents a snapshot of the predator-prey dynamics of  
106 the ultraplankton in this location. The effect of the relatively low abundances of  
107 heterotrophic protists on the accuracy of counts has been examined previously (Martin  
108 et al., 2008) and is not significant enough to affect our results.

109

## 110 2.2 Statistics

111 The Central Limit Theorem provides a straightforward way to estimate the number of  
112 samples that must be taken to obtain a particular level of accuracy for an estimate of  
113 the mean. The one assumption we will make here is that the mean and variance  
114 estimated from our full dataset are the true mean,  $\mu$ , and variance,  $\sigma^2$ , respectively.  
115 Clearly this is an approximation. However, as our dataset comprises greater than 200  
116 points even if it is split into the two halves described later, the difference is likely to  
117 be small. If it is not, then tackling spatial variability is clearly a very major problem.  
118 Given this assumption the estimate of the mean,  $m$ , using  $N$  samples  $X_i$  where  $i=1:N$ ,  
119 has a normal distribution with mean  $\mu$  and variance  $\sigma^2/N$ . Therefore, for example, if  
120 we want to estimate how many points we need to sample to obtain an estimate of the

121 mean within P% of the true mean with 99% probability we simply need to estimate  
122 the number of points to constrain 99% of the distribution for m within  $(1-P/100)*m$   
123 and  $(1+P/100)*m$ . Remember that the distribution of the mean narrows as we increase  
124 N since the variance is  $\sigma^2/N$ .

125

126

### 127 **3. Results**

128

#### 129 *3.1 Large-scale structure*

130 Figure 2 shows the spatial distribution for 6 of the 7 classes of ultraplankton  
131 enumerated, with each coloured spot corresponding to a sample. For phytoplankton,  
132 *Synechococcus*, heterotrophic bacteria and viruses a quick visual analysis might  
133 suggest a strong relationship with temperature and/or physical structures. The eddy  
134 visible as a warm anomaly in the southwest corner (Painter et al., 2007) is  
135 systematically associated with low abundances for all these organisms. However, the  
136 correlations between these organisms and temperature are generally relatively weak  
137 (Figure 3), with the most significant correlation being between viruses and  
138 temperature with a correlation coefficient of -0.66. Similarly weak correlations are  
139 found with salinity and density (not shown). The cause for this weak dependence over  
140 the region as a whole is apparent at the fringes of the survey region. Particularly along  
141 the eastern and northern edges of the survey, organism abundances are as low as  
142 within the eddy.

143 The spatial distribution of large heterotrophic protists (strongly mimicked by  
144 that of small heterotrophic protists which is, therefore, not shown) has little large-  
145 scale structure. Though there are perhaps a few more high abundances within the

146 eddy, similarly high values can be found in all quadrants of the survey. The  
147 correlation coefficient for large heterotrophic protists and temperature is just 0.20  
148 with that for small heterotrophic protists and temperature being 0.38.

149         Regardless of the strength of the relationship between temperature and the  
150 various organisms's abundances, it is clear in Figure 2 that, at least at large scales, the  
151 distributions of phytoplankton, *Synechococcus*, heterotrophic bacteria and viruses  
152 have very similar structure. It is also apparent that this structure is markedly different  
153 to those of the heterotrophic protists. Further evidence for the former point can be  
154 found in the correlation coefficients, shown in Figure 3. The correlation coefficient is  
155 greater than 0.7 for all pairings of phytoplankton groups, *Synechococcus*,  
156 heterotrophic bacteria and viruses. The largest correlation coefficient for any one of  
157 these 5 organisms with either large or small heterotrophic protist groups is -0.25  
158 between *Synechococcus* and large heterotrophic protists. Note that large and small  
159 heterotrophic protists are even uncorrelated with each other (correlation coefficient  
160 equals zero to 2 decimal places).

161         Despite the fact that temperature does not appear to offer an easy explanation  
162 for the organisms' distributions (something reinforced below), there is clear evidence  
163 for a divided community in the area. Figure 4 shows histograms of organisms'  
164 abundance. Phytoplankton and heterotrophic bacteria clearly have bimodal  
165 distributions, strongly suggestive of two different communities in the region. Figure 4  
166 also shows how the abundances are distributed when the samples are split according  
167 to a criterion based on the histogram of the LOP phytoplankton group (see Figure 4  
168 caption). As LOP shows one of the clearest bimodal distributions, with its two peaks  
169 most clearly separated, this organism was used to split the data into two roughly equal  
170 parts: S1 comprising samples where LOP abundance < 8102 cells/ml (208 points) and



171 S2 comprising samples where LOP abundance  $\geq 8102$  cells/ml (211 points). Clearly  
172 this is subjective but there is no objective way to split a bimodal distribution,  
173 particularly in situations such as here where the component ‘peaks’ are both strongly  
174 non-Normal. (Similar results were obtained using the PPH phytoplankton group as a  
175 basis for the split instead.) Splitting in this way suggests a common bimodality, not  
176 just for phytoplankton and heterotrophic bacteria, but also for *Synechococcus* and  
177 viruses. The same split, however, results in no clear demarcation in the distribution of  
178 temperature, once more indicating that it is not the causal factor (similar results hold  
179 for salinity and density though they are not shown). Consistent with the spatial  
180 distributions seen in Figure 2, the two halves of both large and small heterotrophic  
181 protists under the split have near identical histograms (Figure 4). This is consistent  
182 with their spatial distributions, discussed above. In particular there is no evidence for  
183 a bimodal distribution in either large or small heterotrophic protists.

184 Figure 3 shows scatter plots for all pairings of organism abundances and  
185 temperature, with corresponding correlation coefficients at the top of the plot for each  
186 pairing. These plots generally confirm what has already been stated about the  
187 organisms’ spatial variability. The scatter plot of large versus small heterotrophic  
188 protists clearly demonstrates that there is no evidence for two distinct populations for  
189 either of these organisms. Calculating correlation coefficients for samples in each of  
190 the two halves of the split dataset does not increase the magnitude of any of the  
191 coefficients. Looking at some of the relationships exhibited in Figure 3 (e.g. PPH-  
192 SYN or LOP-VIR) one might be tempted to infer evidence of a trajectory associated  
193 with the population dynamics of the region (Srokosz et al., 2003). However, it should  
194 be borne in mind that these ‘trajectories’ link the high abundance cluster in phase  
195 space to that of the low abundances. It may therefore simply be due to mixing of the

196 waters representing the two peaks in the bimodal distribution. We return to this in the  
197 Discussion.

198         Given the bimodal nature of the distributions for several of the organisms and  
199 the reasonable strength of correlation between them it is worth investigating their  
200 spatial distributions in a little more detail. Figure 5 shows the location of samples with  
201 abundances corresponding to the peaks in the histograms for the two phytoplankton  
202 groups, LOP and PPH, shown in Figure 4. For points comprising the lower abundance  
203 peak, LOP and PPH have a broadly similar distribution with some focussed in the  
204 eddy in the southwest corner and others scattered around the northern and eastern  
205 boundaries of the survey region. However, the points comprising the peak in high  
206 abundance can be found primarily in the southeast corner for LOP but primarily in the  
207 northern half for PPH. Hence, though LOP and PPH both display a bimodal  
208 distribution, with each ‘half’ comprising roughly the same sample points, and though  
209 they have a correlation coefficient of 0.81, there is no strong coincidence in the  
210 geographical locations of the samples comprising the two peaks in their abundance  
211 histograms. If one instead focuses on the location of minimum and maximum values  
212 (once more Figure 5), although there is some mismatch with the locations of samples  
213 comprising the peaks in the histograms for each organism, there is still no agreement  
214 between LOP and PPH.

215         The same results were obtained if the bins involved in the histogram in Figure  
216 4 were shifted along by half a bin width.

217

### 218 *3.2 Variability*

219 Having described the spatial variability in the organisms’ distributions we now turn to  
220 how we may accurately estimate the mean abundance of organisms in the area. Our

221 approach to quantifying this has already been explained in the Methods section (2.2).  
222 It should be noted that the following analysis is intended as illustrative. Although  
223 there is no reason to suppose that other regions have less spatial variability than the  
224 site studied, the results we find can only be used as guidelines for other sites. In  
225 particular we are in no way claiming that a bimodal distribution is typical, as this is  
226 likely to arise in only certain situations (see Discussion). However, the dataset, in  
227 revealing two scales of spatial variability – the large scale manifested as the peaks  
228 bimodal distribution and the smaller scale as the distribution about each of the two  
229 peaks – provides an excellent illustration of the dangers of using single or few points  
230 to estimate mean abundances for an area. Figure 6 shows the predicted error in the  
231 mean for a range of sample sizes.

232         Although the temperature histogram shows no evidence of a bimodal  
233 distribution, the predicted errors for the two subsets of data, S1 and S2, are shown  
234 here for comparison – likewise for small and large heterotrophic protists. The  
235 maximum error for temperature is predicted to be largest for S1. This is to be  
236 expected given the longer tail of the distribution for S1 (Figure 4). The error may  
237 seem small at 0.026, but it should be remembered that this is fractional error. Since  
238 the mean temperature for S1 is 15.69 °C, this corresponds to an error of 0.41°C. The  
239 maximum error for S2 is 0.17 °C. To obtain an equally small error for S1 would  
240 require at least 10 samples to be taken.

241         The error curves for S1 and S2 are very similar for both groups of  
242 heterotrophic protist. This is consistent with the unimodal distributions for these  
243 organisms seen in Figure 4. For large heterotrophic protists the largest potential error  
244 is 55% of the true mean, with that for small heterotrophic protists potentially larger

245 than 80%. To bring the likely error for either down to the 25% level would require at  
246 least 10 samples to be taken.

247 All of the remaining organisms (phytoplankton, *Synechococcus*, heterotrophic  
248 bacteria and viruses) have significantly different errors when the mean is estimated  
249 for S1 and S2. In all cases, the wider histogram peak for S1 leads to a larger error than  
250 for S2 using the same sample size. The lowest error is associated with heterotrophic  
251 bacteria for which 10 samples would push the error down to 25% for S1 and almost to  
252 15% for S2. The most extreme errors are associated with *Synechococcus* and viruses  
253 where for S1 errors are still at least as large as 50% even with 10 samples. Although  
254 the presence of a bimodal distribution may be debated for these organisms it should  
255 be noted that regardless of the manner in which the split was carried out the error in  
256 estimated mean associated with either S1 or S2 is still guaranteed to be less than that  
257 obtained using the undivided dataset. For the most clearly bimodally distributed  
258 organisms, corresponding to the two phytoplankton groups, errors for estimating the  
259 mean of S1 are lower than 20% when 10 samples are used. The same number of  
260 samples would give errors of order 40% however for S2.

261 It is worth stressing that bimodality is not the only source of significant  
262 potential error when estimating mean abundances. Even knowing which 'sub-  
263 population' a sample belongs to, so that it can be treated independently as a unimodal  
264 distribution, it is still necessary to have of order 10 samples for an accurate estimate  
265 of the mean.

266 Note that it is more difficult to form estimates of the likely error in estimating  
267 the variance for the organisms' abundances. It is tractable for the mean because the  
268 distribution of mean estimates is Normal. For variance estimates, however, the  
269 distribution is more complicated (Pearson Type III) and no simple guidance can be

270

271

272

273

274

#### 275 **4. Discussion**

276 The data presented here from the D306 cruise cover just 4 days of one year. It is  
277 pertinent to ask how representative these results are of other years and times.

278 Unfortunately, flow cytometers are still far from being a standard instrument on ships,  
279 so few datasets which enumerate the ultraplankton exist for the PAP area. The best  
280 source of data is the UK NERC-funded Atlantic Meridional Transect (AMT)  
281 programme. In particular data are available for AMT13 (September 2003), AMT 16  
282 (June 2005) and AMT 17 (October 2005). There are also data available from the  
283 German Poseidon 300/1 cruise in July 2003. Because these cruises had other  
284 objectives and did not sample the PAP area anywhere near as intensively for  
285 ultraplankton as the D306 cruise, relatively few data are available, even when pooled  
286 from all AMT and Poseidon datasets. Specifically, only *Synechococcus* was counted  
287 on all these previous cruises so we must restrict attention to this organism. Using only  
288 data from the top 20m, to be consistent with the mixed layer data presented here from  
289 D306, we have just 23 previous observations from within our mesoscale survey area  
290 or 49 if we take data from anywhere within the Porcupine Abyssal Plain  
291 (approximately 43-50N 10-20W). If we further insist that the data must have been  
292 collected in the summer (June or July) then these two figures fall to 18 and 30  
293 observations respectively. Hence, we cannot carry out any meaningful statistical  
294 analysis in the manner described above. However, we can at least investigate how

295 these earlier datasets compare to our observations. Figure 7 once more shows the  
296 histogram of abundance for *Synechococcus* but is now superimposed with data from  
297 previous cruises. Previous data from the same area as that mapped by the D306  
298 mesoscale survey show a clear clustering with the peak in high abundances. This is  
299 true whether data are restricted to the summer months to be consistent with D306 or  
300 not. If data are allowed from the broader Porcupine Abyssal Plain area, but restricted  
301 to the summer, this clustering remains. Data from September and October, however,  
302 do contain a number of points of lower abundances. Taking the summer data as  
303 providing the best comparison to D306 data it is tempting to draw the conclusion that  
304 the peak in low abundances seen in the histograms represents a community not  
305 normally present in this area at that time. There is further evidence for this. Painter et  
306 al. (this volume) find evidence for the presence of two distinct water masses in the  
307 region over the course of the cruise. At the time of the mesoscale survey the eddy in  
308 the southwest corner represents a more northerly form of Eastern North Atlantic  
309 Central Water (ENACWp) while the rest of the region is dominated by a southerly  
310 variant (ENACWt) originating from near the Azores. Smythe-Wright et al. (this  
311 volume) find that photosynthetic pigments that can be used as markers for different  
312 types of phytoplankton also reflect this juxtaposition of significantly differing water  
313 masses. Finally, Hartman et al. (this volume) provide evidence that the dominant  
314 water mass in this area may vary from year to year, indicating that the region is one  
315 where the stirring together of markedly different water masses may occur. If the  
316 different water masses have different biogeochemical signatures and different  
317 community structures then the bimodality discussed here may be frequent. Caution is  
318 required, however. First, there are still relatively few observations. Second, it could be  
319 argued that the whole of the D306 dataset is indicative of a different community to

320 previous years. No significant numbers of *Prochlorococcus* cyanobacteria were  
321 detected on D306. Yet on all of the previous cruises mentioned above,  
322 *Prochlorococcus* outnumbered *Synechococcus*. There is currently no understanding of  
323 why *Prochlorococcus* should be absent during D306. Such a dramatic shift does  
324 highlight the need for care in comparing datasets though.

325 From a broader perspective, our data can be compared to recent results from the  
326 shelf seas (Martin et al, 2008). The analysis presented here provides the first open-  
327 ocean evidence of ultraplankton predators being spatially distributed in a significantly  
328 different, essentially more random, manner than their prey. This was exactly the  
329 phenomenon reported by Martin et al. (2008) from the Celtic Sea between UK and  
330 Ireland. Although the bimodal distribution of organisms is very clear for some of the  
331 organisms in Figure 4, this clarity of division is not carried over to their geographical  
332 distributions, and the split between the two communities carries a degree of  
333 subjectivity. Hence, we cannot apply any of the spatial statistical techniques applied  
334 by Martin et al. (2008). Nevertheless our work supports their findings: that  
335 heterotrophic protists can display a significantly different spatial distribution to their  
336 prey. Martin et al. (2008) put forward a hypothesis that top-down pressure, via strong  
337 predation of the heterotrophic protists, could explain this apparent lack of relationship  
338 even in the presence of a strong trophic link between the protists and their prey.  
339 Unfortunately, as in that study, we do not have data on higher predators' abundances  
340 to test this hypothesis. The questions of why viruses were found here to share a  
341 similar distribution to their hosts (most likely LOP) and why large and small  
342 heterotrophic protists had a radically different distribution to their prey must be  
343 addressed by future work.

344 As part of our analysis we make use of standard linear correlations to examine  
345 relationships between different organisms and temperature. A few points are worth  
346 making on this. First, it should be noted that we make no attempt to take into account  
347 possible dependency of neighbouring points – such a dependency can lead to  
348 incorrectly high correlation coefficients. However, to deal with this properly it is  
349 necessary to calculate spatial and temporal auto-correlation scales – only data points  
350 separated by distance and time greater than these two scales respectively should be  
351 used for the calculation of the correlation. We choose not to do this for two reasons.  
352 First, as is clear from the above discussion there is evidence of strongly differing  
353 communities with no clear geographical segregation between them, though with some  
354 evidence of a cause in the juxtaposition and mixing of two different water masses.  
355 This makes the spatial variability in the region strongly non-isotropic. The  
356 autocorrelation scales will therefore vary with position, direction and time, making  
357 such an approach unfeasible. Second, using correlation coefficients to infer an  
358 absence of relationship between heterotrophic protists and their prey is proof against  
359 this issue precisely because correlation analysis will, if anything, make the  
360 relationship look stronger than it really is, so we can have some confidence in a poor  
361 correlation.

362 Taking the dataset presented here in isolation once more, our analysis raises  
363 concerns for how we might approach ecological modelling of the area. It is relatively  
364 straightforward to put together an ecological model – there are a host of previous  
365 formulations that can be used off-the-shelf or combined to give a model of the  
366 required structure provided nothing novel is intended. The greater difficulty lies in  
367 finding sufficient accurate data to constrain the model. This is increasingly important  
368 as the complexity of the model increases, since the number of degrees of freedom to



369 constrain increases. Time-series have long been a stalwart source of data for  
370 constraining models. The provision of data throughout a year allows the model to be  
371 constrained as the ecosystem responds to seasonal changes in forcing. Historically, the  
372 errors reported on data from time-series have been restricted to those arising from  
373 methodology, they have not taken into account spatial variability. This survey has  
374 demonstrated that to obtain an accurate estimate of the mean concentration of a given  
375 organism or group of organisms, it may be necessary to obtain 10 or more samples at  
376 a range of locations. Otherwise, the ‘error’ arising from insufficient sampling of  
377 spatial variability may be much larger than that arising from methodological effects.  
378 This has obvious consequences for models constructed using time-series data.

379

## 380 **5. Conclusions**

381 We have presented high spatial resolution data from a mesoscale survey at the PAP  
382 study site enumerating a range of ultraplankton. Histograms of abundance reveal a  
383 divided community for phytoplankton, prokaryotes, heterotrophic bacteria and  
384 viruses, with two clear groupings. Heterotrophic protists are evenly, if more  
385 randomly, distributed over the whole region. From a practical point of view, we have  
386 further demonstrated that to be able to estimate the mean abundance of some of the  
387 organisms present would require in excess of 10 samples to be taken at different  
388 locations. Without due regard for the spatial variability, it can be a source of greater  
389 variability in observations than observational methodology. There is currently no  
390 reason to think that the PAP site has particularly strong spatial variability relative to  
391 any other open ocean site.

392

## 393 **Acknowledgements**

394 We would like to thank Robin Hankin for statistical advice and the captain and crew  
395 of RRS Discovery for providing such a superb platform for oceanographic research.  
396 This manuscript contributes to the OBE NSRD Oceans 2025 core and AMT  
397 programmes funded by the Natural Environmental Research Council, UK. Adrian  
398 Martin was funded by a NERC Advanced Research Fellowship  
399 (NER/J/S/2001/00708).

400

#### 401 **References**

402

403 Burkill, P.H., 2006. RRS Discovery Cruise 306, 23 Jun - 6 Jul 2006. Pelagic  
404 biogeochemistry of the PAP site. Cruise Report No. 9. National Oceanography Centre,  
405 Southampton, UK.

406

407 Hartman, S.E., Larkin, K.E., Lampitt, R.S., Lankhorst, M. and Hydes, D.J. Seasonal  
408 and inter-annual biogeochemical variations at PAP (49°N 16.5°W) 2003-2005  
409 associated with winter mixing and surface circulation. Deep-Sea Research II, this  
410 volume.

411

412 Jacquet, S., Prieur, L., Avois-Jacquet, C., Lennon, J.F., and Vaultot, D., 2002. Short-  
413 timescale variability of picophytoplankton abundance and cellular parameters in  
414 surface waters of the Alboran Sea (western Mediterranean). Journal of Plankton  
415 Research, 24, 635-651.

416

417 Marie, D., Partensky, F., Jacquet, S. and Vaultot, D., 1997. Enumeration and cell cycle  
418 analysis of natural populations of marine picoplankton by flow cytometry using the  
419 nucleic acid stain SYBR Green I. *Appl. Environ. Microbiol.*, 63, 186-193  
420

421 Martin, A.P., Zubkov, M.V., Burkill, P.H. and Holland, R.J., 2005. Extreme spatial  
422 variability in marine picoplankton and its consequences for interpreting Eulerian time-  
423 series. *Biology Letters*, 1, 366-369.  
424

425 Martin, A.P., Zubkov, M.V., Burkill, P.H. and Holland, R.J., 2008. Microbial spatial  
426 variability: an example from the Celtic Sea. *Progress in Oceanography*, in press.  
427

428 Painter, S.C., Pidcock, R., Allen, J.T., 2007. Mesoscale eddies driving spatial and  
429 temporal heterogeneity in the productivity of the euphotic zone of the NE Atlantic.  
430 *Deep-Sea Research II*, this volume.  
431

432 Smythe-Wright, D., Boswell, S., Kim, Y.-N., Kemp, A.E. Spatio-temporal changes in  
433 the distribution of phytopigments and phytoplanktonic groups at the PAP site. *Deep-  
434 Sea Research II*, this volume.  
435

436 Srokosz, M.A., Martin, A.P. and Fasham, M.J.R., 2003. [On the role of biological  
437 dynamics in plankton patchiness at the mesoscale: an example from the eastern North  
438 Atlantic Ocean.](#) *Journal of Marine Research*, 61, (4), 517-537.  
439

440 Zubkov, M.V., Allen, J.I., and Fuchs, B.M., 2004. Coexistence of dominant groups in  
441 marine bacterioplankton community - a combination of experimental and modelling

442 approaches. *Journal of the Marine Biological Association of the United Kingdom*, 84,  
443 519-529.

444

445 Zubkov, M.V. and Burkill, P.H., 2006. Syringe pumped high speed flow cytometry of  
446 oceanic phytoplankton. *Cytometry Part A*, 69A, 1010-1019.

447

448 Zubkov, M.V., Burkill, P.H., and Topping, J.N., 2007. Flow cytometric enumeration  
449 of DNA-stained oceanic planktonic protists. *Journal of Plankton Research*, 29, 79-86

450

451 Zubkov, M.V. and Quartly, G.D., 2003. Ultraplankton distribution in surface waters  
452 of the Mozambique Channel – flow cytometry and satellite imagery. *Aquatic  
453 Microbial Ecology*, 33, 155-161.

454

455 **FIGURE CAPTIONS**

456

457 **Figure 1.**

458 Map showing location of the mesoscale survey. The ship track during the survey is  
459 shown as a solid line. The four quadrants of the survey are indicated by the dotted  
460 line. Each of the quadrants took one day to complete and were completed in the  
461 following order: northeast, southeast, northwest, southwest. In each case the ship  
462 carried out the ‘radiator’ path before returning to the centre station using the diagonal  
463 ‘dog-leg’.

464

465 **Figure 2.**

466 Spatial distribution of (a) PPH phytoplankton group, (b) large heterotrophic protists,  
467 (c) *Synechococcus*, (d) LOP phytoplankton group, (e) heterotrophic bacteria and (f)  
468 viruses. Each dot corresponds to a sample and the colour of each dot corresponds to  
469  $\log(\text{abundance} + 1)$  where abundance is in cells/ml and log denotes natural logarithm.  
470 The organism abundances are superimposed on contours of temperature (degrees C)  
471 with specific temperatures labelled in a..

472

473 **Figure 3.**

474 Scatter plots for all pairings of  $\log(\text{abundance} + 1)$ , with abundance in units of cells/ml,  
475 for all ultraplankton groups enumerated and temperature (T). Black and grey points  
476 correspond to the split defined in Figure 4. The X-Y labels denote the axes on which  
477 each variable is plotted. TEM corresponds to temperature, BAC stands for  
478 heterotrophic bacteria and VIR represents viruses. All other abbreviations are as in the

479 text. Figures at the top of each subplot denote correlation coefficients for the full  
480 dataset.

481

482 **Figure 4.**

483 Histograms of (a) temperature (degrees C) and  $\log(\text{abundance} + 1)$  where abundance  
484 is in cells/ml for (b) PPH phytoplankton group, (c) large heterotrophic protists, (d)  
485 small heterotrophic protists, (e) *Synechococcus*, (f) LOP phytoplankton group, (g)  
486 heterotrophic bacteria and (h) viruses. The black sections correspond to the fraction of  
487 the histogram comprising samples when  $\log(\text{LOP}+1) < 9$  (or  $\text{LOP} < 8102$  cells/ml). The  
488 grey sections are the remaining fraction. This criterion was chosen by eye to give the  
489 clearest split of the bipolar LOP distribution into 2 separate unipolar distributions.  
490 Similar results are obtained splitting with criterion based on PPH.

491

492 **Figure 5.**

493 Location of samples where abundance of (a) LOP and (b) PPH falls within the  
494 numerically dominant bins for the histograms shown in Figure 4. Black and grey  
495 denote samples within the most abundant bin for the same halves of the dataset  
496 depicted in Figure 4. For LOP this corresponds to  $7.9577 < \log(\text{abundance}+1) < 8.1185$   
497 for black and to  $9.5653 < \log(\text{abundance}+1) < 9.7261$  for grey. For PPH this  
498 corresponds to  $9.2082 < \log(\text{abundance}+1) < 9.3398$  for black and to  
499  $10.2617 < \log(\text{abundance}+1) < 10.3933$  for grey. Abundances are in units of cells/ml.  
500 Squares denote the 20 highest abundances and diamonds the 20 lowest. Also shown  
501 are temperature (degrees C) contours for reference.

502

503 **Figure 6.**

504 Measure of error in estimated mean as a function of the number of samples. The error  
505 is defined as follows. For a given number of samples  $N$ , the error is the value  $Y$  for  
506 which there is a 99% probability that the estimate lies between  $(1-Y)*\mu$  and  $(1+Y)*\mu$   
507 where  $\mu$  is the true mean. For example, a value of  $Y=0.7$  means that the estimate will  
508 be within 70% of the true mean with 99% probability. (a) temperature (degrees C), (b)  
509 PPH phytoplankton group, (c) large heterotrophic protists, (d) small heterotrophic  
510 protists, (e) *Synechococcus*, (f) LOP phytoplankton group, (g) heterotrophic bacteria  
511 and (h) viruses. Solid (low abundances) and dashed (high abundances) lines  
512 correspond to the split defined in Figure 4.

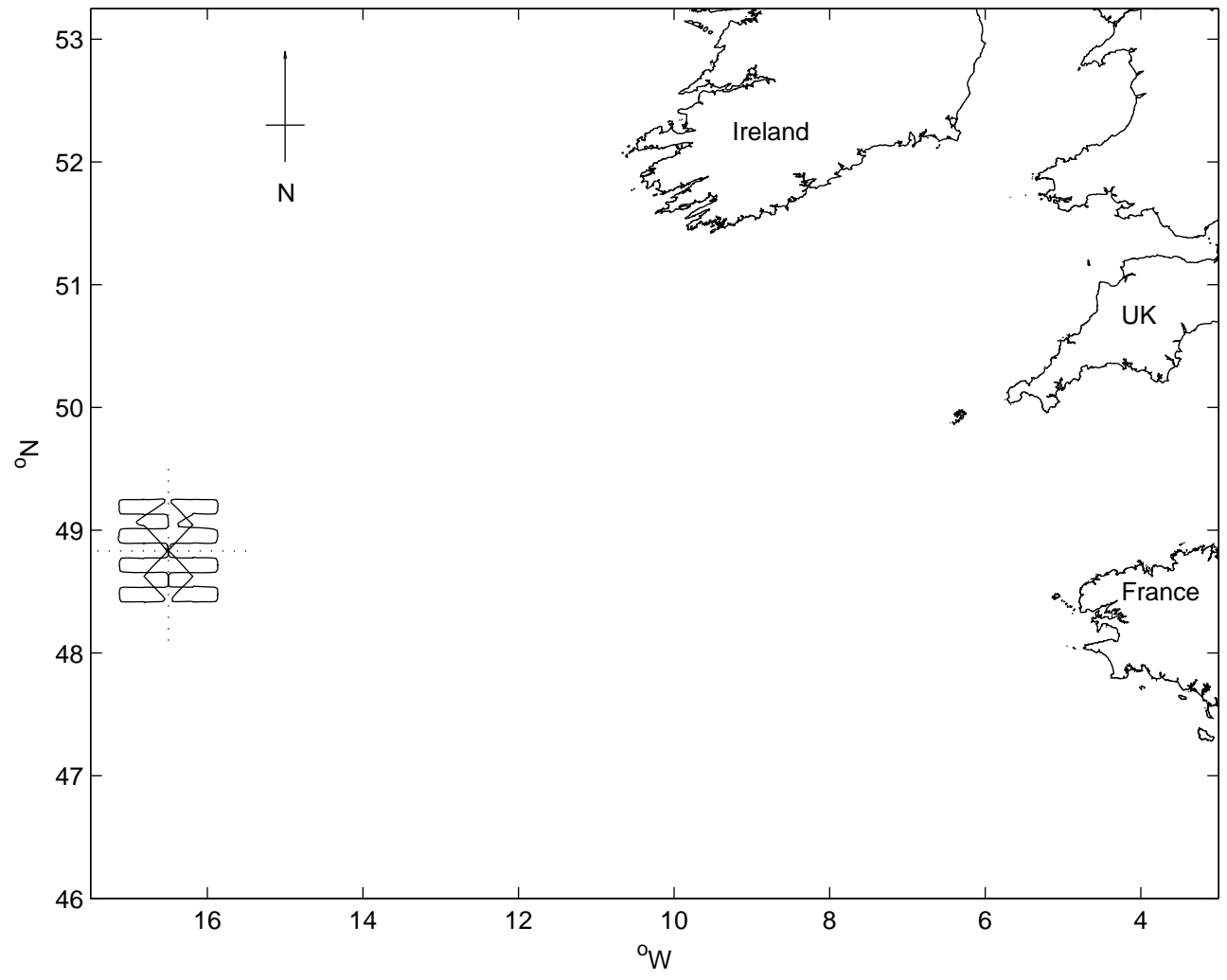
513

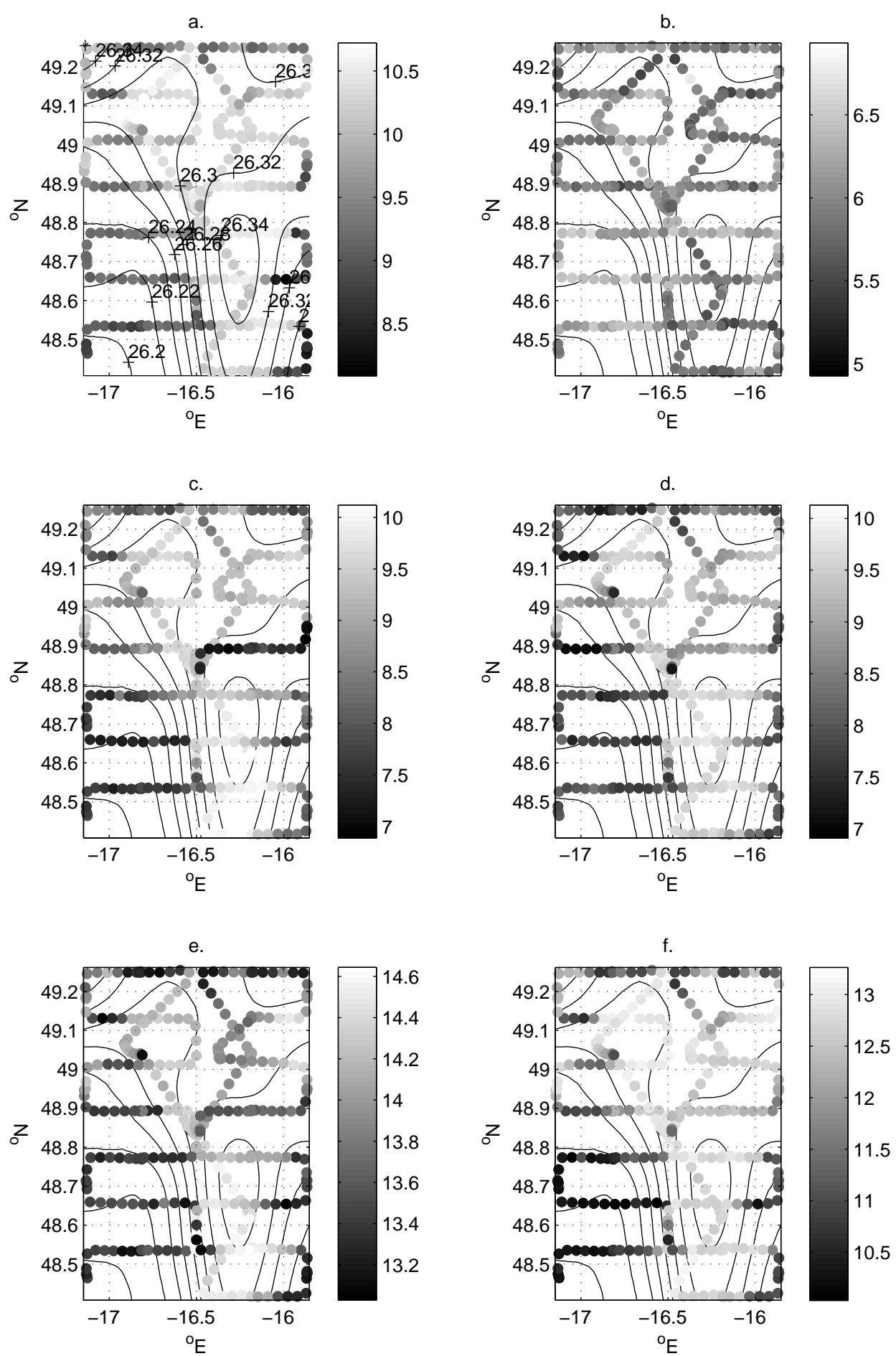
514 **Figure 7.**

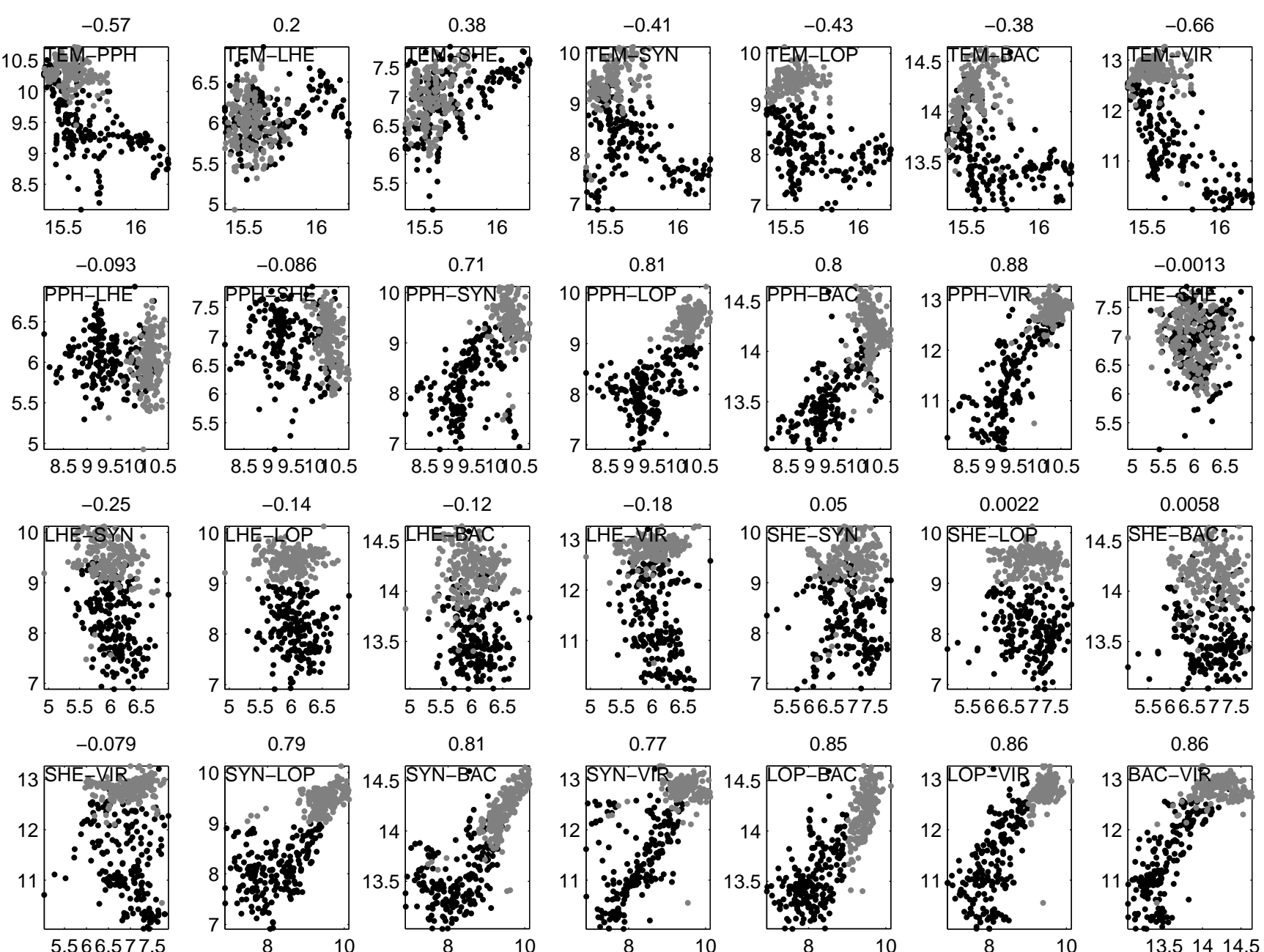
515 Histogram of  $\log(\text{abundance} + 1)$  for *Synechococcus* where abundance is in units of  
516 cells/ml. The split corresponds to that described in the caption to Figure 4, with  
517 black/grey bars corresponding to low/high abundances respectively. Superimposed are  
518 data from AMT13, AMT16, AMT17 and Poseidon 300/1. Squares denote data from  
519 any time of year anywhere within the Porcupine Abyssal Plain, whilst crosses indicate  
520 data from the same area but restricted to June and July. Circles denote previous data  
521 obtained within the boundaries of the D306 mesoscale survey with diamonds the same  
522 data restricted to the months of June and July once more.



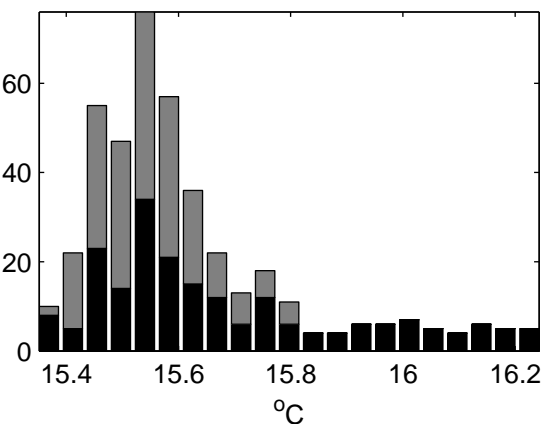




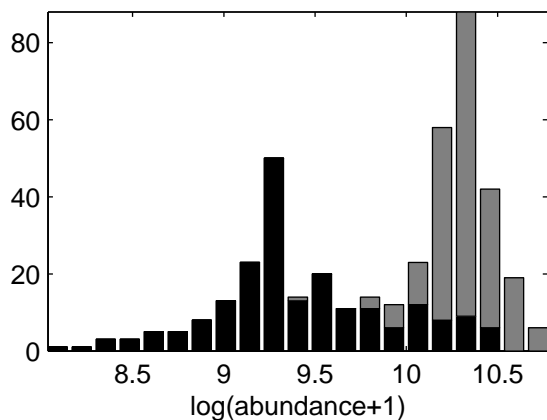




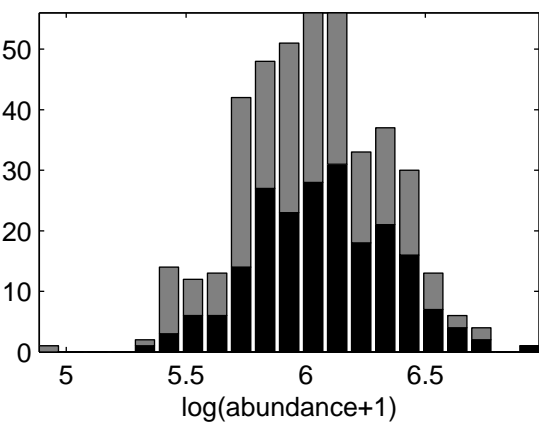
a



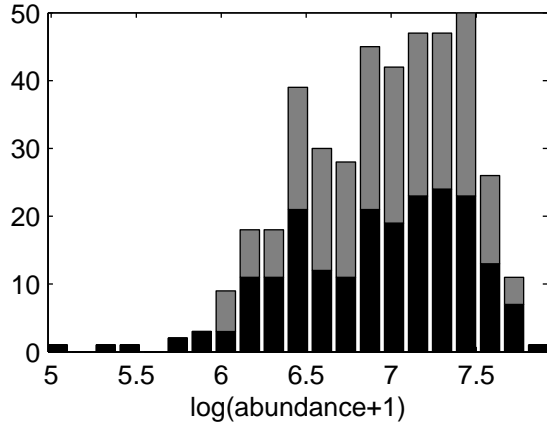
b



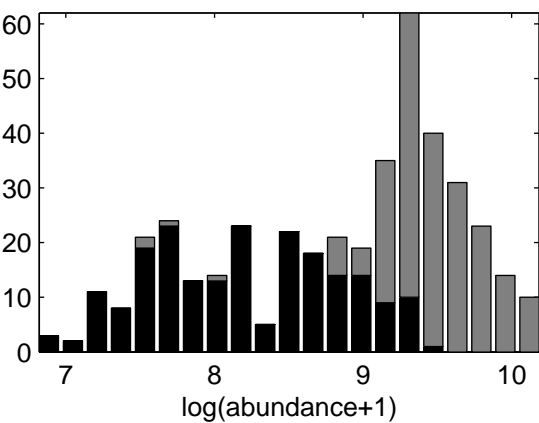
c



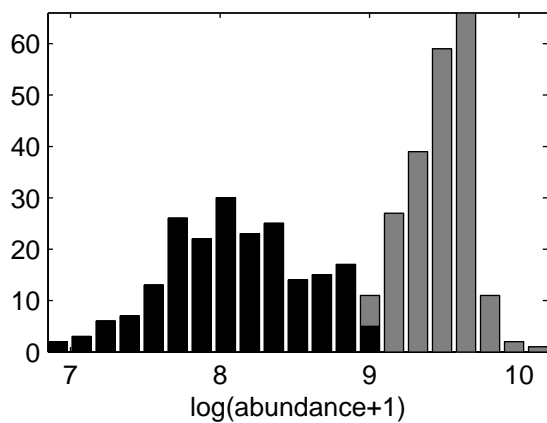
d



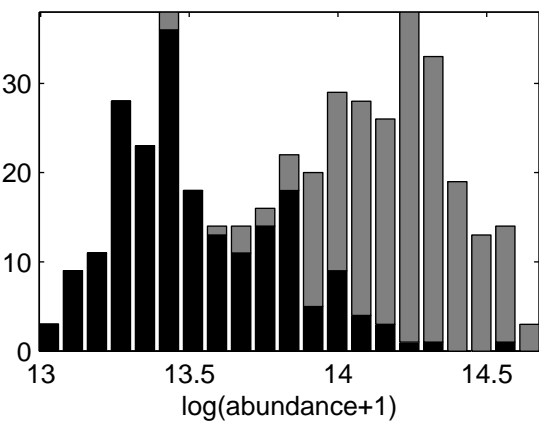
e



f



g



h

